## Collider constraints and new tests of color octet vectors

Malte Buschmann\* and Felix Yu<sup>†</sup>

PRISMA Cluster of Excellence & Mainz Institute for Theoretical Physics,

Johannes Gutenberg University, 55099 Mainz, Germany

We analyze the collider sensitivity for new colored resonances in  $t\bar{t}$ ,  $b\bar{b}$ , and jj final states. While searches in the single production channel are model-dependent, the pair production rate is model independent and the existing (JJ)(JJ) and 4t searches impose strong constraints on the relevant branching fractions, where J=j or b. We point out the missing, complementary searches in the mixed decay modes,  $t\bar{t}(jj)$ ,  $t\bar{t}(b\bar{b})$ , and  $(b\bar{b})(jj)$ . We propose analysis strategies for the  $t\bar{t}(jj)$  and  $t\bar{t}(b\bar{b})$  decays and find their sensivity surpasses that of existing searches when the decay widths to tops and light jets are comparable. If no other decays are present, collective lower limits on the resonance mass can be set at 1.5 TeV using  $37 \text{ fb}^{-1}$  of 13 TeV data.

 $<sup>^{*}</sup>$  buschmann@uni-mainz.de

 $<sup>^{\</sup>dagger}$ yu<br/>001@uni-mainz.de

#### **CONTENTS**

1. Introduction	2
II. Theory background	3
A. Color octet vectors from extended color gauge groups	4
B. Color octet vectors from extra dimensions	5
C. Non-universal couplings and flavor constraints	6
D. Collider phenomenology of color octet vectors	8
III. Collider analyses of the mixed channels, $t\bar{t}(jj)$ and $t\bar{t}(b\bar{b})$	9
A. Event selection strategy	10
B. Comparison with current searches	13
IV. Conclusion	16
Acknowledgments	17
References	17

### I. INTRODUCTION

Searches for new particles and new forces beyond the Standard Model (BSM) are a critical endeavor for the ATLAS and CMS experiments at the Large Hadron Collider (LHC), but such results have thus far come up null. The largest rates come from colored particle pair production, where leading order cross sections can be calculated knowing only the color charge and mass [1]. Even so, the colored particle decay patterns and corresponding collider signatures are highly model dependent.

In models with an extended color gauge symmetry [2–7], massive color octet vectors, such as colorons [8], are heavy cousins of the familiar gluon and can decay universally to Standard Model (SM) quark–anti-quark pairs. Axigluons [4, 9, 10] are similarly motivated by ascribing chiral projection operators to the parent gauge groups, which necessitates new fermions transforming non-trivially under the extended gauge group to cancel anomalies. Similar phenomenology occurs in models of universal extra dimensions, where the massive color octet vectors arise as Kaluza-Klein (KK) excitations of the gluon [11–13]. In Randall-Sundrum models [14, 15] with SM fields propagating in the bulk [16–20], the KK gluons exhibit flavor-dependent couplings to quark pairs,

and preferentially decay to the heavy flavor quarks as a result of the localization of the bulk fermion wavefunction profile [21–25].

At the LHC, CMS and ATLAS have searched for color octet vector resonances in the paired dijet channel [26–31], most recently constraining colorons with a 100% branching fraction to light jets to be heavier than 1.5 TeV [31]. Searches for four tops [32–38] also constrain the possible  $t\bar{t}$  decays of pair-produced resonances. Searches for TeV-scale dijet resonances [39, 40] and  $t\bar{t}$  resonances [41–47] offer complementary probes compared to the pair-production searches, since such searches scale with the individual production coupling [48].

Given the possibility that the color octet vector has flavor dependent branching fractions to quark pairs, and because color octet vectors have a model independent pair production rate, the mixed decay signature of a paired ditop and dijet resonance is strongly motivated. This channel is complementary to the existing (JJ)(JJ) and 4t searches and even offers superior sensitivity when the branching fractions of the resonance to dijets and ditops are comparable.

In Sec. II, we review the theory motivation and collider phenomenology of massive color octet vectors. In Sec. III, we analyze the prospects for discovering color octet vector resonances in the  $t\bar{t}(jj)$  and  $t\bar{t}(b\bar{b})$  mixed decay modes at the LHC and compare with the current constraints. We conclude in Sec. IV.

#### II. THEORY BACKGROUND

Massive color octet vector resonances arise in various different beyond the Standard Model extensions, such as models with extended color gauge groups or models with extra dimensions. In the unbroken phase of electroweak symmetry, the general interaction Lagrangian between quarks and a massive color octet vector  $X_{\mu}$  is

$$\mathcal{L} \supset g_s \left( \bar{Q}_L \gamma_\mu \lambda T^a X^{\mu a} Q_L + \bar{u}_R \gamma_\mu \kappa T^a X^{\mu a} u_R + \bar{d}_R \gamma_\mu T^a \eta X^{\mu a} d_R \right) , \tag{1}$$

where  $g_S$  is the strong coupling constant,  $T^a$  are the SU(3) generators, and  $\lambda$ ,  $\kappa$ , and  $\eta$  are the flavor-dependent couplings in the quark gauge basis. While these matrices must be symmetric by CPT, nonzero off-diagonal entries are possible in principle and correspond to tree-level flavor violation. Since these processes are strongly constrained by low-energy precision flavor measurements, such as meson mixing measurements and  $b \to X_s \gamma$  transitions [49, 50], the simplest ansatz is to adopt a flavor-universal coupling structure, evading the most stringest flavor bounds. In such a scenario, however, the branching ratio for X to light quarks vs. tops is fixed, and there is no model

freedom in the complementarity between searching in dijet vs. ditop resonances. Hence, we will focus on the scenario where the  $\lambda$ ,  $\kappa$ , and  $\eta$  matrices are diagonal but not universal in the quark gauge basis. Moving to the quark mass basis will then induce off-diagonal entries proportional to Cabibbo-Kobayashi-Maskawa (CKM) mixing. We will first briefly review models of massive color octet vectors and then discuss the collider and flavor physics phenomenology of the general Lagrangian, Eq. (1).

#### A. Color octet vectors from extended color gauge groups

In models with an extended color symmetry, such as a  $SU(3)_1 \times SU(3)_2$  gauge group, the two parent gauge groups are typically broken to the diagonal subgroup by the vacuum expectation value (vev) of a bifundamental, complex scalar field  $\Sigma$  [3, 8]. The diagonal subgroup is then identified with the SM  $SU(3)_c$  gauge group, which imposes the requirement

$$\frac{1}{g_s^2} = \frac{1}{h_1^2} + \frac{1}{h_2^2} \,, \tag{2}$$

where  $h_1$  and  $h_2$  are the gauge couplings of  $SU(3)_1$  and  $SU(3)_2$ , respectively. The Goldstone modes of the complex scalar field become the longitudinal degrees of freedom for the heavy color octet vector, leaving one real and one pseudoreal color singlet scalar and one real color octet scalar as the dynamical scalar fields below  $\langle \Sigma \rangle$ . Explicitly, the covariant derivative for  $\Sigma$  is

$$D^{\mu}\Sigma = (\partial^{\mu} - ih_1 G_1^{\mu a} T^a + ih_2 G_2^{\mu a} T^a) \Sigma , \qquad (3)$$

and after Higgsing  $SU(3)_1 \times SU(3)_2 \to SU(3)_c$ , we get the SM gluon and coloron fields,

$$g^{\mu} = \cos \theta \, G_1^{\mu} + \sin \theta \, G_2^{\mu} \, ,$$
  $X^{\mu} = \sin \theta \, G_1^{\mu} - \cos \theta \, G_2^{\mu} \, ,$  (4)

respectively, where  $\theta = \tan^{-1}(h_1/h_2)$  is the mixing angle.

In this setup, different possibilities for the couplings in Eq. (1) originate by considering various charge assignments of the quarks in the parent  $SU(3)_1 \times SU(3)_2$  gauge symmetry. The main feature for universally coupled models is that all flavor representations are assigned identically to the same gauge representation, which ensures that the gauge symmetry commutes with the global SM quark flavor symmetry.

In the coloron model [3, 8], all SM quarks transform as  $\square$  under one SU(3) gauge group and singlets under the other. Hence, the coloron has flavor universal, purely vector couplings to the

SM quarks as

$$g_s \tan \theta \bar{q} \gamma^{\mu} T^a X_{\mu}^a q . \tag{5}$$

An alternative prescription is the chiral color model [4, 9, 51], where left-handed (LH) and right-handed (RH) quark fields are charged under different SU(3) gauge groups. This construction generally requires new fermions to cancel anomalies, notably  $SU(3)_1^2 \times U(1)_Y$  and  $SU(3)_2^2 \times U(1)_Y$ , but this new matter content can be massive and unobservable at colliders. As a result, if the LH quarks transform as  $(\Box, \mathbf{1})$  and the RH quarks transform as  $(\mathbf{1}, \Box)$  under  $SU(3)_1 \times SU(3)_2$ , for example, the resulting massive color vector interaction with quarks is

$$g_s \bar{q} \gamma^{\mu} T^a X^a_{\mu} (\tan \theta P_L - \cot \theta P_R) q , \qquad (6)$$

where  $X^a_{\mu}$  is commonly referred as an axigluon in the literature.

To motivate a non-universal yet diagonal coupling structure in Eq. (1), we can straightforwardly assign different quark flavors to different gauge representations under  $SU(3)_1 \times SU(3)_2$ . For example, the topcolor model charges the third generation quarks differently than the first two generations, with  $Q_L^{1,2} \sim (\Box, \mathbf{1})$ ,  $Q_L^3 \sim (\mathbf{1}, \Box)$ ,  $u_R^{1,2} \sim (\Box, \mathbf{1})$ ,  $u_R^3 \sim (\mathbf{1}, \Box)$ ,  $d_R^{1,2,3} \sim (\Box, \mathbf{1})$  [2]. This assignment also requires additional matter to cancel anomalies, for which a minimal solution involves two electroweak singlet quarks transforming as  $(\mathbf{1}, \Box)$  and  $(\Box, \mathbf{1})$ , each with hypercharge -2/3. The corresponding massive color octet vector does not have flavor-changing couplings in the quark gauge basis, but instead features distinct couplings to light and heavy generation quarks:

$$g_s \cot \theta (\bar{t}\gamma^{\mu} T^a X_{\mu} t + \bar{b}_L \gamma^{\mu} T^a X_{\mu} b_L) + g_s \tan \theta (\bar{b}_R \gamma^{\mu} T^a X_{\mu} b_R + \sum_{i=1...4} \bar{q}_i \gamma^{\mu} T^a X_{\mu} q_i) , \qquad (7)$$

with  $\tan \theta = h_1/h_2$  as before. Although topcolor models are generally motivated by composite Higgs scenarios triggered by top quark condensation [2], we will only focus on the motivated possibility that  $X_{\mu}$  has non-universal couplings.

### B. Color octet vectors from extra dimensions

Models with extra spacetime dimensions provide an alternative framework for realizing massive color octet vector resonances [11–13]. In such models, the SM fields are the lowest-lying states of a Kaluza-Klein tower, whose masses and dynamics result from solving the five-dimensional equations of motion [16–20]. In minimal universal extra dimensions [52], the level-2 KK gluon obtains a coupling to SM quarks from one-loop diagrams with level-1 KK particles running in the

loop. These couplings are generated from boundary conditions on the KK gluon and the bulk masses, which provide the only source of translational invariance breaking, and read

$$g_s T^a \gamma^{\mu} \frac{1}{\sqrt{2}} \frac{1}{16\pi^2} \log \left(\frac{\Lambda}{\mu}\right)^2 \left[ P_L(\frac{1}{8}g_1^2 + \frac{27}{8}g_2^2 - \frac{11}{2}g_s^2) + P_R(Y_{u,d} g_1^2 - \frac{11}{2}g_s^2) \right] , \tag{8}$$

where  $Y_u = 2$  for up-type quarks,  $Y_d = 1/2$  for down-type quarks,  $\Lambda$  is an ultraviolet scale larger than the inverse size of the extra dimension, and  $\mu$  is the renormalization scale to evaluate the coupling.

In Randall-Sundrum warped scenarios [14, 15], the fermion mass hierarchy can be explained by allowing fermions to propagate in the bulk, where the observed charged fermion mass hierarchy originates as  $\mathcal{O}(1)$  differences in bulk mass parameters. Typically, the KK mass scale must then be  $\mathcal{O}(5-10 \text{ TeV})$  to satisfy low-energy flavor violation probes, especially  $\bar{K}-K$  mixing [24], but this scale can be lowered in the case that the bulk fermions obey a flavor symmetry [53, 54]. Since KK parity is absent, the first KK gluon decays to SM zero-mode quarks, and this coupling is given by calculating the wavefunction overlap between the zero modes and the KK gluon in the extra dimension. Using the general coupling structure in Eq. (1) and identifying  $X_{\mu}$  with the first KK gluon,

$$\lambda^{ij} \approx \frac{m_X}{\sqrt{2}M_{KK}} \left( \frac{1}{\sqrt{2L}} \delta_{ij} - \sqrt{2L} F(c_{Q_i}) F(c_{Q_j}) \right) , \qquad (9)$$

where RH up-type couplings are obtained by replacing  $\lambda \to \kappa$  and  $Q \to u$ , RH down-type couplings are obtained by replacing  $\lambda \to \eta$  and  $Q \to d$ ,  $m_X \approx 2.4 M_{\rm KK}$  is fixed by the boundary conditions of the 5D gluon, L is the length of the extra dimension, and  $c_Q$ ,  $c_u$ , and  $c_d$  are the bulk mass parameters for LH and RH quark fields [25]. In order to reproduce the known SM quark masses, these bulk mass parameters must be chosen to maximize the top quark wavefunction overlap with the TeV-scale infrared brane while the wavefunctions for the light quarks are skewed towards the ultraviolet brane. As a result, the first KK gluon preferentially decays to top quarks, with branching fractions that can exceed 80% [25].

### C. Non-universal couplings and flavor constraints

As we have emphasized, massive color octet vectors arise in numerous models of beyond the Standard Model physics. Their collider and flavor physics phenomenology depends crucially on the particular  $\lambda$ ,  $\kappa$ , and  $\eta$  structure defined in Eq. (1) that is realized in a given model. Given the stringent constraints on tree-level flavor changing neutral currents [49, 50], we adopt flavor-diagonal

couplings for  $\lambda$ ,  $\kappa$ , and  $\eta$  in the gauge basis. Nevertheless, flavor violating effects are still induced in interactions of LH down quarks by the rotation to the quark mass basis. From Eq. (1), we rotate the quark fields to the mass basis by  $V_u u_L = u_L^m$ ,  $V_d d_L = d_L^m$ ,  $U_u u_R = u_R^m$ , and  $U_d d_R = d_R^m$ , giving

$$\mathcal{L} \supset \bar{u}_L^m g_s t^a \not X^a V_u \lambda V_u^{\dagger} u_L^m + \bar{d}_L^m g_s t^a \not X^a V_d V_u^{\dagger} V_u \lambda V_u^{\dagger} V_u V_d^{\dagger} d_L^m$$

$$+ \bar{u}_R^m g_s t^a \not X^a U_u \kappa U_u^{\dagger} u_R^m + \bar{d}_R^m g_s t^a \not X^a U_d \eta U_d^{\dagger} d_R^m .$$

$$(10)$$

We see that the  $\lambda$ ,  $\kappa$ , and  $\eta$  matrices can be chosen such that the effective interaction matrices  $\tilde{\lambda}$ ,  $\tilde{\kappa}$ , and  $\tilde{\eta}$  are diagonal in the quark mass basis,

$$\tilde{\lambda} = V_u \lambda V_u^{\dagger} \ , \ \tilde{\kappa} = U_u \kappa U_u^{\dagger} \ , \ \tilde{\eta} = U_d \eta U_d^{\dagger} \ .$$
 (11)

The corresponding LH down quark interactions have small, off-diagonal entries induced by  $V_{CKM} \equiv V_u V_d^{\dagger}$  [55, 56],

$$\tilde{\lambda}_D \equiv V_d V_u^{\dagger} V_u \lambda V_u^{\dagger} V_u V_d^{\dagger} = V_{CKM}^{\dagger} \tilde{\lambda} V_{CKM} , \qquad (12)$$

and hence  $X_{\mu}$  mediates tree-level flavor-changing neutral currents (FCNCs). Since the strongest FCNC constraints come from  $\bar{K}_0 - K_0$  mixing [49], we minimize the impact of these constraints by assuming  $\tilde{\lambda}_{11} = \tilde{\lambda}_{22} \neq \tilde{\lambda}_{33}$ , which leads to  $\tilde{\lambda}_{D,12} \approx \tilde{\lambda}_{D,21} \approx -(3.3 - 1.3i) \times 10^{-4} (\tilde{\lambda}_{33} - \tilde{\lambda}_{11})$ , using global fit values for the CKM elements [56]. A tree-level exchange of  $X_{\mu}$  can be matched to the four-fermion operator [24, 49, 50, 57–59]

$$O_K^1 = (\bar{d}_\alpha \gamma_\mu P_L s_\alpha)(\bar{d}_\beta \gamma^\mu P_L s_\beta) , \qquad (13)$$

with the Wilson coefficient

$$C_K^1 = \frac{-1}{6} \frac{\tilde{\lambda}_{D,12}^2}{M_X^2} \ . \tag{14}$$

Using the requirement  $\Lambda > 1.1 \times 10^3$  TeV from Re  $C_K^1$  and  $\Lambda > 2.2 \times 10^4$  TeV from Im  $C_K^1$  [49], we can constrain the maximum size of  $\tilde{\lambda}_{11}$ ,  $\tilde{\lambda}_{33}$ , assuming the other is vanishing:

Re 
$$C_K^1$$
:  $M_X > 130 \text{ GeV} g_s \max(|\tilde{\lambda}_{11}|, |\tilde{\lambda}_{33}|)$  (15)

Im 
$$C_K^1$$
:  $M_X > 2700 \text{ GeV} g_s \max(|\tilde{\lambda}_{11}|, |\tilde{\lambda}_{33}|)$ . (16)

We see that these constraints are easily satisfied for  $\mathcal{O}(\text{TeV})$  scale color octets as long as  $\tilde{\lambda} \sim \mathcal{O}(0.1)$ . Moreover, with this structure,  $\tilde{\lambda}_{11} = \tilde{\lambda}_{22}$ , the stronger constraints come from  $\bar{B}_d^0 - B_d^0$  and  $\bar{B}_s^0 - B_s^0$  measurements, where  $|C_{B_d}^1|$  requires  $\Lambda > 1.0 \times 10^3$  TeV and  $|C_{B_s}^1|$  requires  $\Lambda > 240$  TeV. Using the tree-level, CKM-induced off-diagonal elements of  $\tilde{\lambda}_D$ , we obtain

$$|C_{B_d}^1|: M_X > 3500 \text{ GeV} g_s \max(|\tilde{\lambda}_{11}|, |\tilde{\lambda}_{33}|)$$
 (17)

$$|C_{B_s}^1|: M_X > 4000 \text{ GeV} g_s \max(|\tilde{\lambda}_{11}|, |\tilde{\lambda}_{33}|),$$
 (18)

which are again weakened to the sub-TeV scale for  $\tilde{\lambda} \sim \mathcal{O}(0.1)$ . As a result, we can realistically expect  $\mathcal{O}(\text{TeV})$  color octet vectors with dominant branching fractions to either tops,  $\tilde{\lambda}_{33} \gg \tilde{\lambda}_{11}$  or jets,  $\tilde{\lambda}_{11} \gg \tilde{\lambda}_{33}$ , entirely consistent with flavor bounds. We remark that an alternative assumption of the flavor structure can relax these bounds further. In particular, if instead  $V_{CKM}^{\dagger} \tilde{\lambda} V_{CKM}$  is diagonal, then the tree-level flavor violating couplings are shifted to the LH up-quark couplings [57, 58]. We can define  $\tilde{\lambda}' = V_{CKM}^{\dagger} \tilde{\lambda} V_{CKM}$  as diagonal, and then the LH up-quark couples via  $V_{CKM} \tilde{\lambda}' V_{CKM}^{\dagger}$ , which is constrained by  $D_0 - \bar{D}_0$  mixing, where  $\Lambda > 700$  TeV [49]. The corresponding bound is

Im 
$$C_D^1$$
:  $M_X > 36 \text{ GeV} g_s \max(|\tilde{\lambda}_{11}|, |\tilde{\lambda}_{33}|)$ . (19)

The  $\Delta F = 1$  constraints, including  $b \to X_s \gamma$  and  $b \to X_s g$  penguin amplitudes, are also immediately satisfied if the  $X^{\mu}$  couplings are aligned in the down-quark sector [50, 58].

## D. Collider phenomenology of color octet vectors

Color octet vectors can be singly and doubly produced at colliders. The single-production rate scales with the corresponding partial width into  $q\bar{q}$ , q=d,u,s,c, since single production via gluons is forbidden at tree-level. In our scenario, the induced flavor-violating couplings  $\tilde{\lambda}_D$  are at most  $5\% \times \tilde{\lambda}_{11}, \tilde{\lambda}_{33}$ , which we will neglect and hence approximate  $\tilde{\lambda}_D \approx \tilde{\lambda}$ . The partial width of X to a pair of quarks q is

$$\Gamma(X \to \bar{q}q) = \frac{\alpha_s m_X}{12} \left( (g_L^2 + g_R^2)(1 - \frac{m_q^2}{m_X^2}) + 6\frac{m_q^2}{m_X^2} g_L g_R \right) \left( 1 - 4\frac{m_q^2}{m_X^2} \right)^{1/2} , \qquad (20)$$

where  $g_L$  and  $g_R$  are the corresponding diagonal entries in  $\tilde{\lambda}$ ,  $\tilde{\kappa}$ , and  $\tilde{\eta}^1$ . If the masses of the quarks can be neglected compared to the X mass, the partial width simplifies to

$$\Gamma(X \to \bar{q}q) = \frac{\alpha_s(g_L^2 + g_R^2)m_X}{12} \ . \tag{22}$$

$$\Gamma(X \to \bar{q}_i q_j, \bar{q}_j q_i) = \frac{\alpha_s m_X}{6} \left( ((g_L^{ij})^2 + (g_R^{ij})^2) (1 - \frac{1}{2} (\frac{m_i^2}{m_X^2} + \frac{m_j^2}{m_X^2}) - \frac{1}{2} (\frac{m_i^2}{m_X^2} - \frac{m_j^2}{m_X^2})^2) + 6 \frac{m_i m_j}{m_X^2} g_L^{ij} g_R^{ij} \right) \\
\times \left( (1 - \frac{m_i^2}{m_X^2} - \frac{m_j^2}{m_X^2})^2 - 4 \frac{m_i^2 m_j^2}{m_X^4} \right)^{1/2}, \tag{21}$$

where  $g_L^{ij} = g_L^{ji}$  and  $g_R^{ij} = g_R^{ji}$ .

<sup>&</sup>lt;sup>1</sup> For reference, the generalized flavor violating partial width is

The branching fractions for jj,  $b\bar{b}$ , and  $t\bar{t}$  final states are then simply ratios of the corresponding sum of squared couplings. We see that large branching fractions to top quarks can easily be realized by increasing  $\tilde{\kappa}_{33}$ , while large branching fractions to bottom quarks corresponds to increasing  $\tilde{\eta}_{33}$ . This is the effective description of the warped extra dimension scenario with  $t_R$  and  $b_R$  wavefunction profiles peaked close to the infrared brane [25], and small hierarchies in these third generation couplings are consistent with electroweak precision tests [57, 58].

As previously highlighted, the single dijet resonance constraints scale with the overal partial width into light flavor quarks. Pair-production rates, however, are robustly calculable knowing only  $m_X$  and its color octet representation. Hence, all searches in pair-production modes provide important complementary reach compared to single resonance searches. The current LHC analyses focus on the simplest topologies, with  $XX^* \to (JJ)(JJ)$ , with J=j or b inclusively [26–31] and  $XX^* \to 4t$  [32–38]. In the case where the  $X \to b\bar{b}$  decay width is preferred, additional signal discrimination is easily gained by requiring b-tags. The orthogonal  $(b\bar{b})(b\bar{b})$ ,  $(b\bar{b})(jj)$ , and (jj)(jj) signal regions would then have enhanced and complementary sensitivity compared to the current (JJ)(JJ) searches. If the coupling to tops is preferred, then the 4t search and our proposed searches in the  $t\bar{t}(jj)$  and  $t\bar{t}(b\bar{b})$  mixed decay channels are critical. In particular, the  $t\bar{t}(jj)$  and  $t\bar{t}(b\bar{b})$  mixed decay searches offer substantial improvements in covering the sensitivity gap when the X decay widths to tops and light quarks are comparable. In the next section, we describe our collider analyses optimized for the  $t\bar{t}(jj)$  and  $t\bar{t}(b\bar{b})$  final states.

### III. COLLIDER ANALYSES OF THE MIXED CHANNELS, $t\bar{t}(jj)$ AND $t\bar{t}(b\bar{b})$

We analyze pair-produced resonances in a new mixed decay mode,  $pp \to XX^* \to t\bar{t}(jj)$  and  $pp \to XX^* \to t\bar{t}(b\bar{b})$ . Although there are numerous possibilities for the top decays, we mainly focus on the semi-leptonic and fully leptonic final states, which provide clean handles for tagging the reconstructible  $t\bar{t}$  and dijet systems. Of course, the main SM background is the irreducible  $t\bar{t}$  jets background, where other single boson and diboson + jets backgrounds are subleading after requiring multiple b-jets.

We construct a FeynRules v2.3.26 [60] model using Universal FeynRules Output [61] to perform leading order Monte Carlo event simulation with MADGRAPH 5 v2.4.3 [62], interfaced with Pythia v8.2 [63, 64] for showering and hadronizations. We remark that the leading order calculation allows a direct comparison to existing (JJ)(JJ) and 4t search limits [26–38]. Since the signal will rely on tagging two top candidates, we simulate the SM background,  $t\bar{t}j$  with up to two

additional jets at leading order, using Sherpa v.2.1.0 [65]. We rescale the background by a flat K-factor of 1.5, adopted from Sherpa+BlackHat [65, 66]. The inclusive SM  $t\bar{t}$  + jets production cross section is known at next-to-next-to-leading order and next-to-next-to-leading log (NNLL) precision [67], whereas differential cross sections can be obtained at next-to-leading order and NNLL precision [68]. Since our X resonance should appear as a resonant peak over a smooth continuum background, a  $p_T$ -dependent K-factor should not significantly affect our projected results.

# A. Event selection strategy

We first discuss the semi-leptonic top decay channel, where our signal process is  $XX^* \to b\bar{b}\ell^{\pm}\nu jj(JJ)$ , with J=j or b. Jets are clustered using the anti- $k_T$  algorithm [69] with R=0.5, and we require jets to have  $p_T>50$  GeV and  $|\eta|<4.9$ . We identify b-jets using a Delphes v3.1.2 [70] detector simulation, with a  $p_T$ - and  $\eta$ -dependent tagging efficiency of about 70% for displaced tracks from B-mesons within  $\Delta R<0.3$  from the main jet axis; the charm misidentification rate is roughly 15% and the light flavor mistag rate is 0.1%.

Events must have at least 5 jets, at least two of which must be b-tagged and one must be untagged. The leading b-tagged and untagged jets must have  $p_T \geq 250$  GeV, and the subleading untagged jet, if present, must have  $p_T \geq 80$  GeV. Events must also have exactly one isolated lepton with  $p_T > 20$  GeV and  $|\eta| < 2.5$ , with isolation using Delphes default parameters. We furthermore cut on missing transverse energy (MET), requiring  $E_T > 80$  GeV, as well as signal mass-optimized  $H_T = \Sigma_j |p_{T,j}| \geq (4/3) m_X$ .

Naively, the  $X \to JJ$  signal resonance is extracted from forming the invariant mass of the two leading jets. The jet combinatorics, however, present a major hurdle against using the dijet and ditop masses to discriminate the signal from the irreducible background. Thus, the main goal of our collider strategy is to solve the combinatorial ambiguity, taking advantage of the resonant high mass dijet signal, the large  $p_T$  of the resonant dijet system, and the relevant angular spread between the b-jets, lepton, and jets. Difficulties in resolving multijet combinatorial ambiguities are discussed in, e.g., [71].

For this purpose, we define two signal regions. We target the  $b\bar{b}$  mode by selecting events with more than two b-tagged jets, while the jj mode is optimized by requiring exactly two b-tagged jets. For the  $b\bar{b}$  decay, we assume that the leading b-tagged jet comes from the  $X \to JJ$  decay directly, not from  $t\bar{t}$ . We then reconstruct the  $b\bar{b}$  system by adding the remaining leading jet, whether tagged or untagged. We find that this reconstruction best reflects the dijet resonance in spite of

Semi-Leptonic Search	Signal			Background $t\bar{t}$ +jets		
Signal mass $m_X$	1.3  TeV	$1.5~{\rm TeV}$	$1.7~{\rm TeV}$	1.3 TeV	$1.5~{\rm TeV}$	$1.7~{ m TeV}$
Event selection [fb] $(N_J \ge 5 \text{ with } N_j \ge 1, N_b \ge 2;$						
$N_{\ell} = 1; p_{T,j}^{\text{leading}}, p_{T,b}^{\text{leading}} > 250 \text{ GeV}; p_{T,\ell} > 20 \text{ GeV}$	1.52	0.45	0.13	5.8	5.8	5.8
$E_T > 80 \text{ GeV}$	84%	87%	89%	64%	64%	64%
$H_T \ge (4/3)  m_X$	83%	79%	76%	32%	19%	10%
Remaining cross section [fb]	1.06	0.31	0.09	1.23	0.71	0.39

TABLE I. Cut flow for different resonance masses  $m_X$  and dominant background  $t\bar{t}$ +jets for the semileptonic search. All branching ratios are applied to signal and background when quoting cross sections. We normalize the signal assuming  $\text{Br}(X \to t\bar{t}) = \text{Br}(X \to JJ) = 50\%$ .

the underlying combinatorial ambiguity.

For the jj mode, we start with the leading light jet  $j_1$  and add to it the hardest light jet  $j_2$  which satisfies  $\Delta R_{j_1j_2} \leq \pi$ . We also add in the next hardest light jet  $j_3$  with  $\Delta R_{j_1j_3} \leq \pi$  if  $j_1$  and  $j_2$  are not balanced in  $p_T$ , when  $p_{T,j_2}/p_{T,j_1} \leq 0.15$ . This follows the hemisphere intuition, where the  $X \to jj$  decays should be untagged and relatively hard. Adding the third hardest light jet accounts for the wide-angle final state radiation of our signal quarks.

For both bb and jj decay modes, we construct the dijet invariant mass as our final kinematic discriminant. The signal and background cut efficiencies for the semileptonic analysis are shown in Table I, while the most salient kinematic distributions for the background stacked with different signal hypotheses are shown in Fig. 1. The upper left panel in Fig. 1 shows the hardening of the  $H_T$  distribution coming from the signal jets. The dijet  $p_{T,JJ}$  distribution, however, only offers an overal rate shift from the additional signal events and no strong correlation with the signal X mass, which is because of the combinatorial ambiguity among the jets. The bottom panels show the invariant mass distributions in the jj and  $b\bar{b}$  targetted modes. Again, the broad peak structure arises mostly from the combinatorial ambiguity in capturing the correct signal jets to reconstruct the resonance. We note that b-tagging efficiency and the combinatorial ambiguity also cause  $X \to jj$  events to populate the  $m_{bb}$  signal region and vice versa.

The search in the fully leptonic top quark decay channel is very similar. We again select jets and leptons as in the semi-leptonic channel, but we require only 4 jets, at least two of which are b-tagged, and also require exactly two isolated leptons of opposite charge. We loosen the MET cut,  $E_T > 50$  GeV, and keep the  $H_T$  cut,  $H_T \ge (4/3) m_X$ . To avoid the anticipated Z+jets

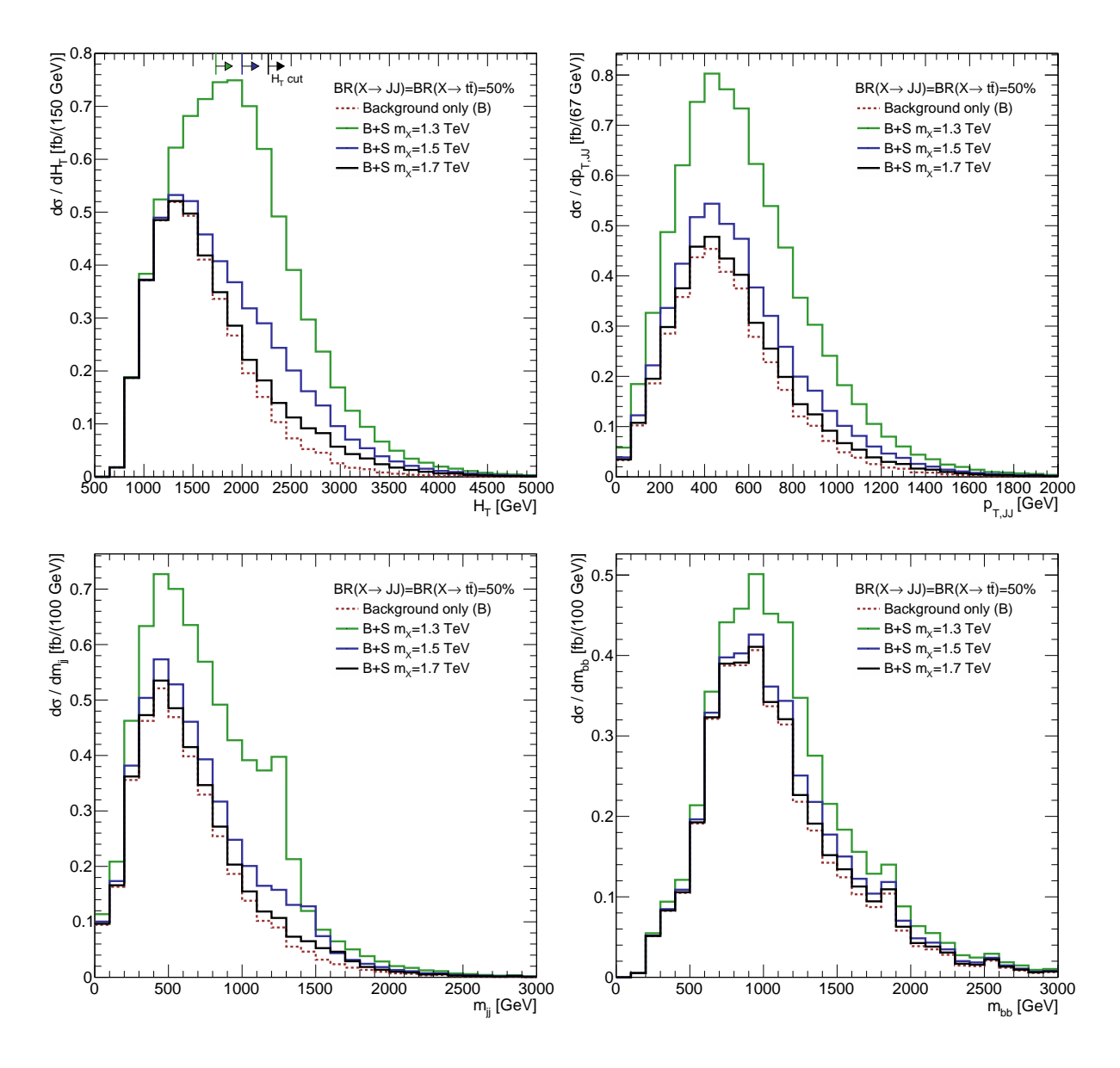


FIG. 1. Differential distributions in the semi-leptonic analysis for  $H_T$  (upper left),  $p_{T,JJ}$  (upper right),  $m_{jj}$  (lower left), and  $m_{bb}$  (lower right), where the invariant mass definitions are described in the main text. We show distributions for the SM  $t\bar{t}$ + jets background (red, dashed), stacked background +  $m_X = 1.3$  TeV signal (green, solid), background +  $m_X = 1.5$  TeV signal (blue, solid), background +  $m_X = 1.7$  TeV signal (black, solid). Differential distributions are presented after jet selection and  $E_T$  cuts but before the  $H_T$  to show the unsculpted dijet invariant mass spectra.

background we veto events with  $m_{\ell\ell} \leq 115$  GeV. Again we distinguish between  $b\bar{b}$  and jj dijet resonance decay modes, using the same method as the semi-leptonic search. The corresponding cut flow is presented in Table II. The final signal rates lead to the same relative signal to background ratios as the semi-leptonic analysis, but the absolute rate is only an  $\approx 5\%$  additional contribution

compared to the semi-leptonic channel.

Fully Leptonic Search	Signal			Background $t\bar{t}$ +jets		
Signal mass $m_X$	1.3  TeV	$1.5~{\rm TeV}$	$1.7~{\rm TeV}$	1.3  TeV	$1.5~{\rm TeV}$	$1.7~{\rm TeV}$
Event selection [fb] $(N_J \ge 4 \text{ with } N_b \ge 2;$						
$N_{\ell} = 2; p_{T,j}^{\text{leading}}, p_{T,b}^{\text{leading}} > 250 \text{ GeV}; p_{T,\ell} > 20 \text{ GeV}$	0.148	0.045	0.009	0.75	0.75	0.75
$E_T > 50 \text{ GeV}$	96%	96%	97%	91%	91%	91%
$m_{\ell\ell} \ge 115 \text{ GeV}$	66%	68%	70%	37%	37~%	37%
$H_T \ge (4/3)  m_X$	63%	57%	48%	21%	11%	2.7%
Remaining cross section [fb]	0.059	0.017	0.003	0.053	0.027	0.007

TABLE II. Cut flow for a different resonance masses  $m_X$  and dominant background  $t\bar{t}$ +jets for the fully leptonic search. All branching ratios are applied to signal and background when quoting cross sections. We normalize the signal assuming  $Br(X \to t\bar{t}) = Br(X \to JJ) = 50\%$ .

# B. Comparison with current searches

We now compare the projected sensitivity from the mixed  $t\bar{t}(JJ)$  searches in combination with the recasted exclusions from ATLAS and CMS for (JJ)(JJ) and 4t searches. We also show the single production limits for dijet and ditop resonance searches. Since we assume that our new physics state X only decays to quark pairs, we can express the pair production constraints in the branching fraction vs. mass plane, where

$$Br(X \to t\bar{t}) = 1 - Br(X \to JJ)$$
 (23)

So, the pair production limits can be translated according to:

$$\sigma_{\text{excl}}(JJ)(JJ)|_{m_X} = \sigma(pp \to XX^*)|_{m_X} \times (\text{Br}_{JJ})^2 ,$$
 (24)

with  $\operatorname{Br}_{JJ} = \operatorname{Br}(X \to JJ)$ . The 4t constraint and the  $t\bar{t}(JJ)$  projected exclusion after replacing  $(\operatorname{Br}_{JJ})^2$  with  $(\operatorname{Br}_{tt})^2$  and  $2(\operatorname{Br}_{JJ}\operatorname{Br}_{tt})$ , respectively, where  $\operatorname{Br}_{tt} = \operatorname{Br}(X \to t\bar{t})$ .

The single dijet resonance limits are determined only after specifying the total width of the resonance. If the total width is narrow, a reference cross section can be rescaled by the partial width into light quarks. We see that

$$\sigma_{\text{excl}}(pp \to (JJ)_{\text{res}})|_{m_X} = \sigma_{\text{width}} \operatorname{Br}_{JJ} A = \sigma_{\text{ref}} \operatorname{Br}_{JJ}^2 \frac{\Gamma_{\text{tot, width}}}{\Gamma_{qq, \text{ref}}} A$$
 (25)

In the case of  $t\bar{t}$  resonances, the above constraint becomes a bounded requirement on the branching fraction to tops. Hence, the  $t\bar{t}$  resonance constraint follows

$$\sigma_{\text{excl}}(pp \to (t\bar{t})_{\text{res}})|_{m_X} \ge \sigma_{\text{width}} \operatorname{Br}_{tt} = \sigma_{\text{ref}}(1 - \operatorname{Br}_{tt}) \operatorname{Br}_{tt} \frac{\Gamma_{\text{tot, width}}}{\Gamma_{qq,\text{ref}}}$$
 (26)

Note that here we drop the acceptance factor since the experiments unfold the acceptance when presenting their results. We combine all four orthogonal signal regions of the semi-leptonic and fully leptonic search and compute the 95% C.L. limits based on the respective JJ invariant mass shapes, where we assume a 10% systematic uncertainty on signal and background. The result can be found in Fig. 2.

We remark that the width of our resonance,  $\Gamma_X = 5 \times 10^{-4} m_X$ , corresponds to diagonal entries of  $\tilde{\lambda}$ ,  $\tilde{\kappa}$ ,  $\tilde{\eta} \lesssim 0.1$ . As discussed in Subsec. II C, such LH quark couplings to X readily satisfy flavor violation bounds from meson oscillation measurements and neutral current transitions given  $m_X > 1$  TeV. On the other hand, these couplings generally arise from mixing the SM quarks with heavy vectorlike states, since otherwise perturbativity in the parent extended color gauge symmetry is violated [48]. The corresponding flavor violation bounds, collider constraints, electroweak precision observable tests are more model-dependent, but realistic and complete scenarios can be constructed [50, 57, 58].

As mentioned previously, the sensitivity from single production compared to the sensitivity from pair production strongly depends on the ratio  $\Gamma_X/m_X$ . Any direct resonance bounds from JJ searches could in principle be evaded completely with a suitably small choice of  $\Gamma_X$ , but choosing  $\Gamma_X/m_X = 5 \times 10^{-4}$  allows complementary dijet constraints from CMS and ATLAS [39, 40]. We remark that the  $t\bar{t}$  resonance limits [47] are absent from Fig. 2 for  $\Gamma_X/m_X = 5 \times 10^{-4}$ . These constraints are only relevant once  $\Gamma_X/m_X \gtrsim 7 \times 10^{-4}$  for  $m_X$  around 1 TeV. As shown in Eq. (26), the  $t\bar{t}$  resonance limit is symmetric around  $\mathrm{Br}_{tt} = 50\%$  since the maximum rate in this channel corresponds to equal partial widths to dijets and ditops.

The strongest existing bounds in Fig. 2 are therefore from (JJ)(JJ) [31] and 4t [38] searches, which are clearly optimal for their respective  $Br_{JJ}$  and  $Br_{tt}$  corners. The mass reach of both searches weakens by about 250 GeV in the intermediate regime, however, leaving significant room for our dedicated  $t\bar{t}(JJ)$  search to explore.

In Fig. 2, we assume that all quark couplings are flavour universal except for the top. We relax this assumption in Fig. 3, allowing both branching fractions  $Br(X \to b\bar{b}) = Br_{bb}$  and  $Br_{tt}$  to float. The results are presented in an equilateral triangle since the sum of the jj,  $b\bar{b}$  and  $t\bar{t}$  branching fractions must equal 100% in our model. The shading in the left panel of Fig. 3 shows the lower

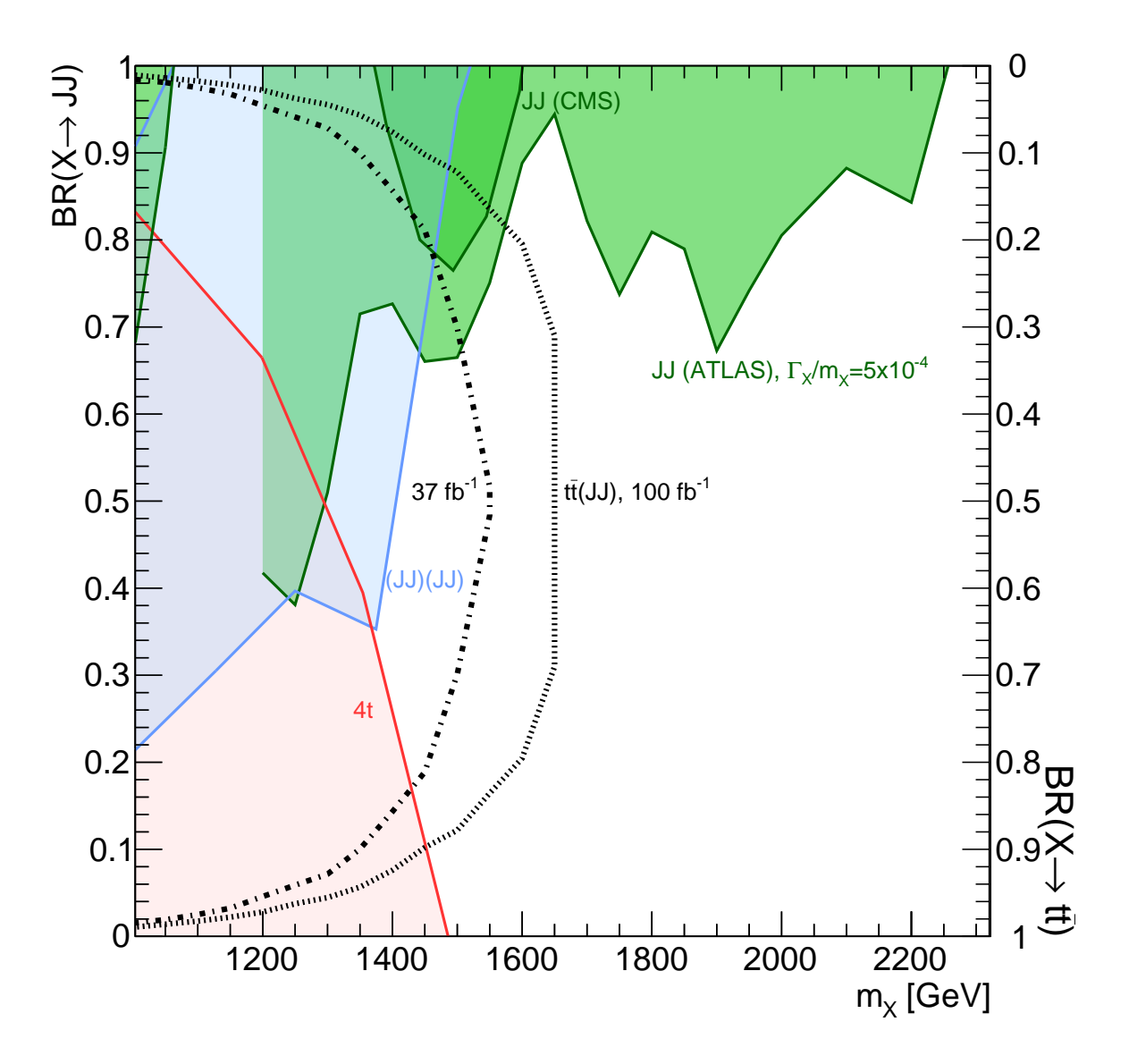


FIG. 2. Exclusion limits for different resonance masses as a function of  $Br(X \to JJ) = 1 - Br(X \to t\bar{t})$ . We show our limit in black for 37 fb<sup>-1</sup> (dot-dashed) and 100 fb<sup>-1</sup> (dashed) of integrated luminosity. We also show current limits from 4t (red) [38], (JJ)(JJ) (blue) [31], and (JJ) (green) [39, 40] searches.

limit on the resonance mass  $m_X$  as a function of the three branching fractions. The right panel of Fig. 3 indicates which particular dedicated search yields the corresponding lower mass limit. We see that our new search channels,  $t\bar{t}(jj)$  and  $t\bar{t}(b\bar{b})$ , overtake the sensitivity in the central areas of the triangle compared to the existing (JJ)(JJ) and 4t searches.

We reiterate that a complete characterization of  $t\bar{t}$ ,  $b\bar{b}$ , and jj decay channels for pair production colored resonances would necessitate optimizing the current (JJ)(JJ) search into  $(b\bar{b})(b\bar{b})$ ,  $(b\bar{b})(jj)$ , and (jj)(jj) signal regions. In particular, the  $(b\bar{b})(b\bar{b})$  search would bear striking similarities with

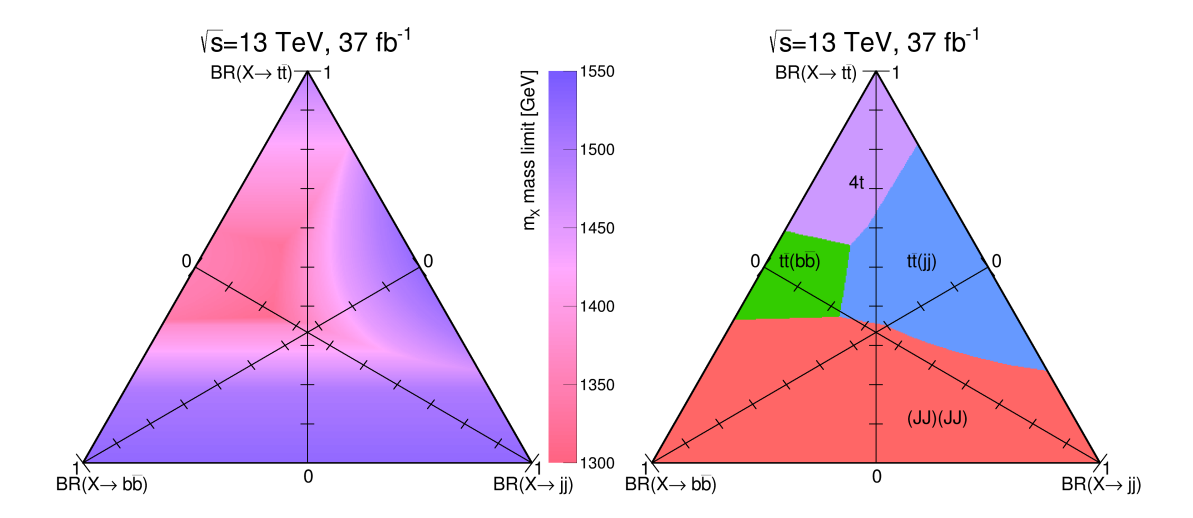


FIG. 3. Left: Strongest mass limits when the various  $t\bar{t}$ ,  $b\bar{b}$ , and jj decay channels are compared. Right: Search region that gives the best sensitivity.

the current searches for pair production of the 125 GeV Higgs [72, 73], where the main novelty would be varying the  $(b\bar{b})$  mass window to test for new resonances. The multijet background, however, is very challenging to simulate and thus substantial statistics in the *b*-tagged backgrounds would be required to suitably smooth paired invariant mass spectrum in the  $(b\bar{b})(b\bar{b})$  and  $(b\bar{b})(jj)$  channels.

### IV. CONCLUSION

In this work, we have highlighted the  $t\bar{t}(jj)$  and  $t\bar{t}(b\bar{b})$  mixed decay channels of a massive, color octet vector as new targets for ATLAS and CMS searches. Hierarchies in the underlying couplings of the X resonance to light quarks, bottom pairs, or top pairs are entirely consistent with low energy FCNC constraints if the X mass is above 1 TeV and its couplings to quarks are at most 0.1. As a result, the LHC provides the leading reach to TeV-scale color octet vectors with variable couplings to heavy and light flavor quarks by virtue of the model independent pair production rate.

In our  $t\bar{t}(JJ)$  analyses, we focused on resolving the jet combinatorial ambiguity to reconstruct the dijet or dibottom resonance. In principle, reconstructing the  $(t\bar{t})$  resonance is also possible, but our scenario with its many resolved jets did not afford any additional signal discrimination in this regard.

Nevertheless, our results show that new  $t\bar{t}(jj)$  and  $t\bar{t}(b\bar{b})$  searches will fill a sensitivity gap between the (JJ)(JJ) and 4t searches. This gap is clear in the  $\text{Br}_{JJ}$  vs.  $m_X$  plane, which itself provides a useful tool for easily presenting the results from different collider searches of pairproduced resonances. We stress that a post-discovery scenario of a new resonance greatly benefits from this complementary information, where single and pair production modes combined with different decay channels provide direct information about underlying Lagrangian couplings.

#### ACKNOWLEDGMENTS

FY would like to thank R. Sekhar Chivukula and Elizabeth Simmons for helpful discussions during the 2015 Les Houches summer session, and also Susanne Westhoff at the Mainz Institute for Theoretical Physics, "The TeV Scale: A Threshold to New Physics?" 2017 scientific program. FY would also like to acknowledge the hospitality of the theory group at Fermi National Accelerator Laboratory while this work was completed. This research is supported by the Cluster of Excellence Precision Physics, Fundamental Interactions and Structure of Matter (PRISMA-EXC 1098). The work of MB is moreover supported by the German Research Foundation (DFG) in the framework of the Research Unit "New Physics at the Large Hadron Collider" (FOR 2239).

<sup>[1]</sup> Tao Han, Ian Lewis, and Zhen Liu, "Colored Resonant Signals at the LHC: Largest Rate and Simplest Topology," JHEP **12**, 085 (2010), arXiv:1010.4309 [hep-ph].

<sup>[2]</sup> Christopher T. Hill, "Topcolor: Top quark condensation in a gauge extension of the standard model," Phys. Lett. B266, 419–424 (1991).

<sup>[3]</sup> R. S. Chivukula, Andrew G. Cohen, and Elizabeth H. Simmons, "New strong interactions at the Tevatron?" Phys. Lett. **B380**, 92–98 (1996), arXiv:hep-ph/9603311 [hep-ph].

<sup>[4]</sup> Paul H. Frampton and Sheldon L. Glashow, "Chiral Color: An Alternative to the Standard Model," Phys. Lett. B190, 157–161 (1987).

<sup>[5]</sup> M. V. Martynov and A. D. Smirnov, "Chiral color symmetry and possible G-prime-boson effects at the Tevatron and LHC," Mod. Phys. Lett. A24, 1897–1905 (2009), arXiv:0906.4525 [hep-ph].

<sup>[6]</sup> Paul H. Frampton, Jing Shu, and Kai Wang, "Axigluon as Possible Explanation for  $p\bar{p} \to t\bar{t}$  Forward-Backward Asymmetry," Phys. Lett. **B683**, 294–297 (2010), arXiv:0911.2955 [hep-ph].

<sup>[7]</sup> Elizabeth H. Simmons, R. Sekhar Chivukula, Baradhwaj Coleppa, Heather E. Logan, and Adam Martin, "Topcolor in the LHC Era," in *Proceedings, KMI Inauguration Conference on Quest for the Origin of Particles and the Universe (KMIIN): Nagoya, Japan, October 24-26, 2011* (2011) pp. 237–251, arXiv:1112.3538 [hep-ph].

<sup>[8]</sup> Yang Bai and Bogdan A. Dobrescu, "Heavy octets and Tevatron signals with three or four b jets," JHEP 07, 100 (2011), arXiv:1012.5814 [hep-ph].

<sup>[9]</sup> Lawrence J. Hall and Ann E. Nelson, "Heavy Gluons and Monojets," Phys. Lett. B153, 430 (1985).

- [10] Jonathan Bagger, Carl Schmidt, and Stephen King, "Axigluon Production in Hadronic Collisions," Phys. Rev. D37, 1188 (1988).
- [11] Thomas Appelquist, Hsin-Chia Cheng, and Bogdan A. Dobrescu, "Bounds on universal extra dimensions," Phys. Rev. **D64**, 035002 (2001), arXiv:hep-ph/0012100 [hep-ph].
- [12] Thomas G. Rizzo, "Probes of universal extra dimensions at colliders," Phys. Rev. D64, 095010 (2001), arXiv:hep-ph/0106336 [hep-ph].
- [13] C. Macesanu, C. D. McMullen, and S. Nandi, "Collider implications of universal extra dimensions," Phys. Rev. D66, 015009 (2002), arXiv:hep-ph/0201300 [hep-ph].
- [14] Lisa Randall and Raman Sundrum, "A Large mass hierarchy from a small extra dimension," Phys. Rev. Lett. 83, 3370-3373 (1999), arXiv:hep-ph/9905221 [hep-ph].
- [15] Lisa Randall and Raman Sundrum, "An Alternative to compactification," Phys. Rev. Lett. 83, 4690–4693 (1999), arXiv:hep-th/9906064 [hep-th].
- [16] H. Davoudiasl, J. L. Hewett, and T. G. Rizzo, "Bulk gauge fields in the Randall-Sundrum model," Phys. Lett. B473, 43–49 (2000), arXiv:hep-ph/9911262 [hep-ph].
- [17] Yuval Grossman and Matthias Neubert, "Neutrino masses and mixings in nonfactorizable geometry," Phys. Lett. **B474**, 361–371 (2000), arXiv:hep-ph/9912408 [hep-ph].
- [18] Alex Pomarol, "Gauge bosons in a five-dimensional theory with localized gravity," Phys. Lett. **B486**, 153–157 (2000), arXiv:hep-ph/9911294 [hep-ph].
- [19] Sanghyeon Chang, Junji Hisano, Hiroaki Nakano, Nobuchika Okada, and Masahiro Yamaguchi, "Bulk standard model in the Randall-Sundrum background," Phys. Rev. D62, 084025 (2000), arXiv:hep-ph/9912498 [hep-ph].
- [20] Stephan J. Huber and Qaisar Shafi, "Fermion masses, mixings and proton decay in a Randall-Sundrum model," Phys. Lett. B498, 256–262 (2001), arXiv:hep-ph/0010195 [hep-ph].
- [21] D. A. Dicus, C. D. McMullen, and S. Nandi, "Collider implications of Kaluza-Klein excitations of the gluons," Phys. Rev. **D65**, 076007 (2002), arXiv:hep-ph/0012259 [hep-ph].
- [22] H. Davoudiasl, J. L. Hewett, and T. G. Rizzo, "Experimental probes of localized gravity: On and off the wall," Phys. Rev. D63, 075004 (2001), arXiv:hep-ph/0006041 [hep-ph].
- [23] Ben Lillie, Lisa Randall, and Lian-Tao Wang, "The Bulk RS KK-gluon at the LHC," JHEP 09, 074 (2007), arXiv:hep-ph/0701166 [hep-ph].
- [24] S. Casagrande, F. Goertz, U. Haisch, M. Neubert, and T. Pfoh, "Flavor Physics in the Randall-Sundrum Model: I. Theoretical Setup and Electroweak Precision Tests," JHEP 10, 094 (2008), arXiv:0807.4937 [hep-ph].
- [25] Kaustubh Agashe, Martin Bauer, Florian Goertz, Seung J. Lee, Luca Vecchi, Lian-Tao Wang, and Felix Yu, "Constraining RS Models by Future Flavor and Collider Measurements: A Snowmass Whitepaper," (2013), arXiv:1310.1070 [hep-ph].
- [26] Serguei Chatrchyan et al. (CMS), "Search for pair-produced dijet resonances in four-jet final states in pp collisions at  $\sqrt{s}$ =7 TeV," Phys. Rev. Lett. **110**, 141802 (2013), arXiv:1302.0531 [hep-ex].

- [27] Vardan Khachatryan et al. (CMS), "Search for pair-produced resonances decaying to jet pairs in proton collisions at  $\sqrt{s} = 8$  TeV," Phys. Lett. **B747**, 98–119 (2015), arXiv:1412.7706 [hep-ex].
- [28] CMS Collaboration (CMS), "Search for low-mass pair-produced dijet resonances using jet substructure techniques in proton-proton collisions at a center-of-mass energy of  $\sqrt{s} = 13$  TeV," (2016).
- [29] Georges Aad et al. (ATLAS), "Search for pair-produced massive coloured scalars in four-jet final states with the ATLAS detector in proton-proton collisions at  $\sqrt{s} = 7$  TeV," Eur. Phys. J. C73, 2263 (2013), arXiv:1210.4826 [hep-ex].
- [30] The ATLAS collaboration (ATLAS), "A search for pair produced resonances in four jets final states in proton-proton collisions at  $\sqrt{s}$ =13 TeV with the ATLAS experiment," (2016).
- [31] The ATLAS collaboration (ATLAS), "A search for pair-produced resonances in four-jet final states at  $\sqrt{s} = 13$  TeV with the ATLAS detector," (2017).
- [32] CMS Collaboration (CMS), "Search for standard model four top quark production at 8 TeV in the lepton + jets channel," (2013).
- [33] Albert M Sirunyan *et al.* (CMS), "Search for standard model production of four top quarks in protonproton collisions at  $\sqrt{s} = 13$  TeV," (2017), arXiv:1702.06164 [hep-ex].
- [34] "Search for exotic same-sign dilepton signatures (b' quark,  $T_{5/3}$  and four top quarks production) in 4.7 fb<sup>-1</sup> of pp collisions at  $\sqrt{s} = 7$  TeV with the ATLAS detector," (2012).
- [35] Georges Aad et al. (ATLAS), "Search for production of vector-like quark pairs and of four top quarks in the lepton-plus-jets final state in pp collisions at  $\sqrt{s} = 8$  TeV with the ATLAS detector," JHEP **08**, 105 (2015), arXiv:1505.04306 [hep-ex].
- [36] The ATLAS collaboration, "Search for production of vector-like top quark pairs and of four top quarks in the lepton-plus-jets final state in pp collisions at  $\sqrt{s} = 13$  TeV with the ATLAS detector," (2016).
- [37] The ATLAS collaboration (ATLAS), "Search for four-top-quark production in final states with one charged lepton and multiple jets using 3.2 fb<sup>-1</sup> of proton-proton collisions at  $\sqrt{s} = 13$  TeV with the ATLAS detector at the LHC," (2016).
- [38] The ATLAS collaboration (ATLAS), "Search for new phenomena in  $t\bar{t}$  final states with additional heavy-flavour jets in pp collisions at  $\sqrt{s} = 13$  TeV with the ATLAS detector," (2016).
- [39] CMS Collaboration (CMS), "Searches for dijet resonances in pp collisions at  $\sqrt{s} = 13$  TeV using data collected in 2016." (2017).
- [40] Morad Aaboud et al. (ATLAS), "Search for new phenomena in dijet events using 37 fb<sup>-1</sup> of pp collision data collected at  $\sqrt{s}$  =13 TeV with the ATLAS detector," (2017), arXiv:1703.09127 [hep-ex].
- [41] Serguei Chatrchyan et al. (CMS), "Search for resonant  $t\bar{t}$  production in lepton+jets events in pp collisions at  $\sqrt{s} = 7$  TeV," JHEP 12, 015 (2012), arXiv:1209.4397 [hep-ex].
- [42] Serguei Chatrchyan et al. (CMS), "Search for Z 'resonances decaying to  $t\bar{t}$  in dilepton+jets final states in pp collisions at  $\sqrt{s}=7$  TeV," Phys. Rev. **D87**, 072002 (2013), arXiv:1211.3338 [hep-ex].
- [43] Georges Aad et al. (ATLAS), "A search for  $t\bar{t}$  resonances in lepton+jets events with highly boosted top quarks collected in pp collisions at  $\sqrt{s} = 7$  TeV with the ATLAS detector," JHEP **09**, 041 (2012),

- arXiv:1207.2409 [hep-ex].
- [44] Georges Aad et al. (ATLAS), "Search for resonances decaying into top-quark pairs using fully hadronic decays in pp collisions with ATLAS at  $\sqrt{s} = 7$  TeV," JHEP **01**, 116 (2013), arXiv:1211.2202 [hep-ex].
- [45] Georges Aad et al. (ATLAS), "Search for  $t\bar{t}$  resonances in the lepton plus jets final state with ATLAS using 4.7 fb<sup>-1</sup> of pp collisions at  $\sqrt{s}=7$  TeV," Phys. Rev. **D88**, 012004 (2013), arXiv:1305.2756 [hep-ex].
- [46] Georges Aad et al. (ATLAS), "A search for  $t\bar{t}$  resonances using lepton-plus-jets events in proton-proton collisions at  $\sqrt{s} = 8$  TeV with the ATLAS detector," JHEP **08**, 148 (2015), arXiv:1505.07018 [hep-ex].
- [47] The ATLAS collaboration, "Search for heavy particles decaying to pairs of highly-boosted top quarks using lepton-plus-jets events in proton-proton collisions at  $\sqrt{s} = 13$  TeV with the ATLAS detector," (2016).
- [48] Bogdan A. Dobrescu and Felix Yu, "Coupling-mass mapping of dijet peak searches," Phys. Rev. **D88**, 035021 (2013), [Erratum: Phys. Rev. D90,no.7,079901(2014)], arXiv:1306.2629 [hep-ph].
- [49] M. Bona et al. (UTfit), "Model-independent constraints on ΔF = 2 operators and the scale of new physics," JHEP 03, 049 (2008), see update 'Unitarity Triangle analysis beyond the Standard Model from UTfit,' by Marcella Bona at ICHEP 2016, August 5, 2016, Chicago. Accessed June, 9, 2017 from http://utfit.org/UTfit/References, arXiv:0707.0636 [hep-ph].
- [50] R. Sekhar Chivukula, Elizabeth H. Simmons, and Natascia Vignaroli, "A Flavorful Top-Coloron Model," Phys. Rev. D87, 075002 (2013), arXiv:1302.1069 [hep-ph].
- [51] Paul H. Frampton and Sheldon L. Glashow, "Unifiable Chiral Color With Natural Gim Mechanism," Phys. Rev. Lett. 58, 2168 (1987).
- [52] AseshKrishna Datta, Kyoungchul Kong, and Konstantin T. Matchev, "Minimal Universal Extra Dimensions in CalcHEP/CompHEP," New J. Phys. 12, 075017 (2010), arXiv:1002.4624 [hep-ph].
- [53] Mu-Chun Chen, K. T. Mahanthappa, and Felix Yu, "A Viable Randall-Sundrum Model for Quarks and Leptons with T-prime Family Symmetry," Phys. Rev. D81, 036004 (2010), arXiv:0907.3963 [hep-ph].
- [54] Mu-Chun Chen, K. T. Mahanthappa, and Felix Yu, "A Viable Flavor Model for Quarks and Leptons in RS with T-prime Family Symmetry," Proceedings, 7th International Conference on Supersymmetry and the Unification of Fundamental Interactions (SUSY09): Boston, USA, June 5-10, 2009, AIP Conf. Proc. 1200, 623–626 (2010), arXiv:0909.5472 [hep-ph].
- [55] Oram Gedalia and Gilad Perez, "Flavor Physics," in Physics of the large and the small, TASI 09, proceedings of the Theoretical Advanced Study Institute in Elementary Particle Physics, Boulder, Colorado, USA, 1-26 June 2009 (2011) pp. 309–382, arXiv:1005.3106 [hep-ph].
- [56] C. Patrignani et al. (Particle Data Group), "Review of Particle Physics," Chin. Phys. C40, 100001 (2016).
- [57] Yang Bai, JoAnne L. Hewett, Jared Kaplan, and Thomas G. Rizzo, "LHC Predictions from a Tevatron Anomaly in the Top Quark Forward-Backward Asymmetry," JHEP 03, 003 (2011), arXiv:1101.5203 [hep-ph].

- [58] Ulrich Haisch and Susanne Westhoff, "Massive Color-Octet Bosons: Bounds on Effects in Top-Quark Pair Production," JHEP **08**, 088 (2011), arXiv:1106.0529 [hep-ph].
- [59] Wolfgang Altmannshofer, Reinard Primulando, Chiu-Tien Yu, and Felix Yu, "New Physics Models of Direct CP Violation in Charm Decays," JHEP 04, 049 (2012), arXiv:1202.2866 [hep-ph].
- [60] Adam Alloul, Neil D. Christensen, Cline Degrande, Claude Duhr, and Benjamin Fuks, "FeynRules 2.0
   A complete toolbox for tree-level phenomenology," Comput. Phys. Commun. 185, 2250–2300 (2014), arXiv:1310.1921 [hep-ph].
- [61] Celine Degrande, Claude Duhr, Benjamin Fuks, David Grellscheid, Olivier Mattelaer, and Thomas Reiter, "UFO - The Universal FeynRules Output," Comput. Phys. Commun. 183, 1201–1214 (2012), arXiv:1108.2040 [hep-ph].
- [62] J. Alwall, R. Frederix, S. Frixione, V. Hirschi, F. Maltoni, O. Mattelaer, H. S. Shao, T. Stelzer, P. Torrielli, and M. Zaro, "The automated computation of tree-level and next-to-leading order differential cross sections, and their matching to parton shower simulations," JHEP 07, 079 (2014), arXiv:1405.0301 [hep-ph].
- [63] Torbjorn Sjostrand, Stephen Mrenna, and Peter Z. Skands, "A Brief Introduction to PYTHIA 8.1," Comput. Phys. Commun. 178, 852–867 (2008), arXiv:0710.3820 [hep-ph].
- [64] Torbjrn Sjstrand, Stefan Ask, Jesper R. Christiansen, Richard Corke, Nishita Desai, Philip Ilten, Stephen Mrenna, Stefan Prestel, Christine O. Rasmussen, and Peter Z. Skands, "An Introduction to PYTHIA 8.2," Comput. Phys. Commun. 191, 159–177 (2015), arXiv:1410.3012 [hep-ph].
- [65] T. Gleisberg, Stefan. Hoeche, F. Krauss, M. Schonherr, S. Schumann, F. Siegert, and J. Winter, "Event generation with SHERPA 1.1," JHEP 02, 007 (2009), arXiv:0811.4622 [hep-ph].
- [66] C. F. Berger, Z. Bern, L. J. Dixon, F. Febres Cordero, D. Forde, H. Ita, D. A. Kosower, and D. Maitre, "An Automated Implementation of On-Shell Methods for One-Loop Amplitudes," Phys. Rev. D78, 036003 (2008), arXiv:0803.4180 [hep-ph].
- [67] Michal Czakon, Paul Fiedler, and Alexander Mitov, "Total Top-Quark Pair-Production Cross Section at Hadron Colliders Through  $O(\alpha_s^4)$ ," Phys. Rev. Lett. **110**, 252004 (2013), arXiv:1303.6254 [hep-ph].
- [68] Marco Guzzi, Katerina Lipka, and Sven-Olaf Moch, "Top-quark pair production at hadron colliders: differential cross section and phenomenological applications with DiffTop," JHEP 01, 082 (2015), arXiv:1406.0386 [hep-ph].
- [69] Matteo Cacciari, Gavin P. Salam, and Gregory Soyez, "The Anti-k(t) jet clustering algorithm," JHEP 04, 063 (2008), arXiv:0802.1189 [hep-ph].
- [70] J. de Favereau, C. Delaere, P. Demin, A. Giammanco, V. Lematre, A. Mertens, and M. Selvaggi (DELPHES 3), "DELPHES 3, A modular framework for fast simulation of a generic collider experiment," JHEP 02, 057 (2014), arXiv:1307.6346 [hep-ex].
- [71] Arvind Rajaraman and Felix Yu, "A New Method for Resolving Combinatorial Ambiguities at Hadron Colliders," Phys. Lett. **B700**, 126–132 (2011), arXiv:1009.2751 [hep-ph].

- [72] Morad Aaboud et al. (ATLAS), "Search for pair production of Higgs bosons in the  $b\bar{b}b\bar{b}$  final state using proton–proton collisions at  $\sqrt{s}=13$  TeV with the ATLAS detector," Phys. Rev. **D94**, 052002 (2016), arXiv:1606.04782 [hep-ex].
- [73] CMS Collaboration (CMS), "Search for non-resonant pair production of Higgs bosons in the bbbb final state with 13 TeV CMS data," (2016).